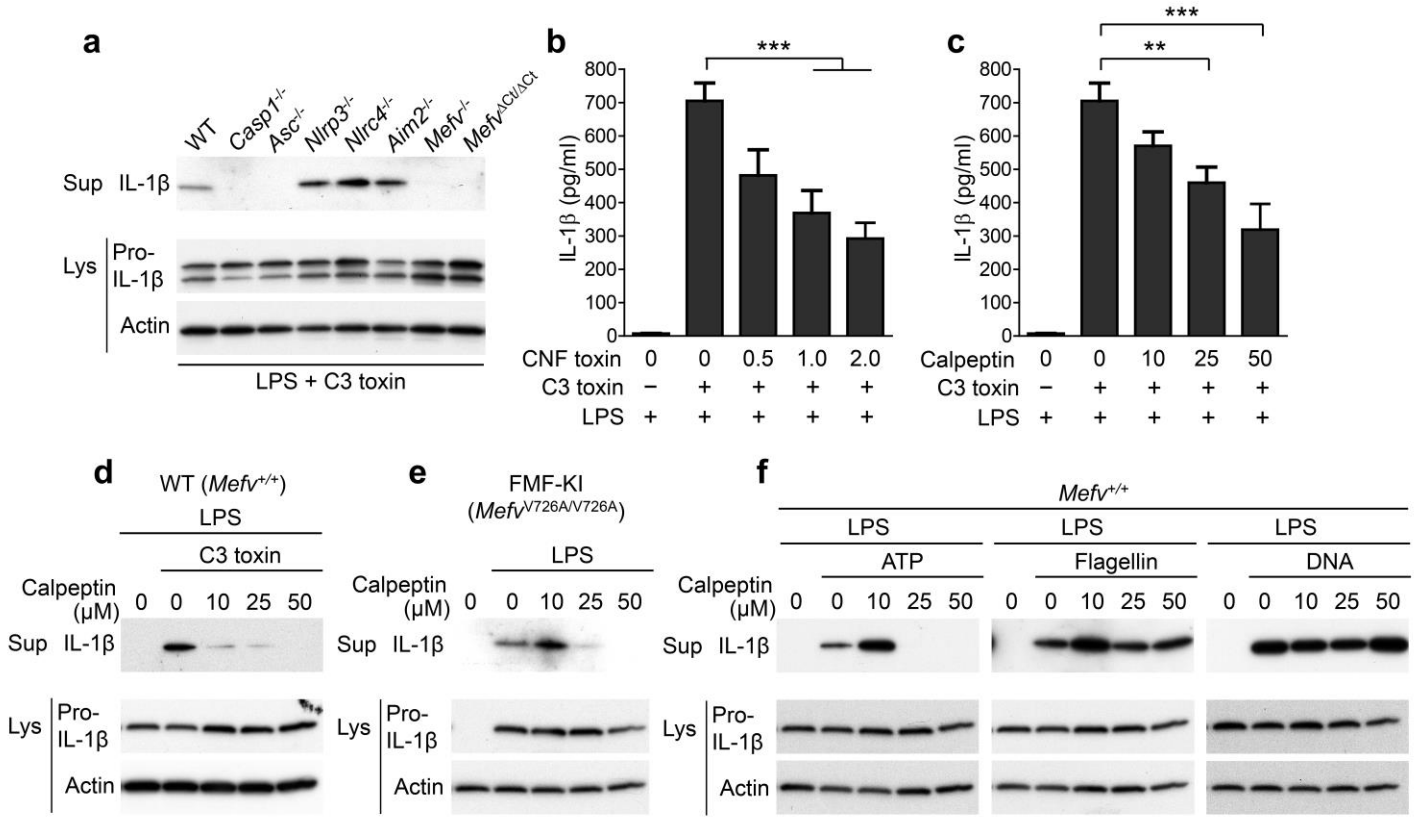

Supplementary Figure 1

The pyrin inflammasome is activated by inactivation of RhoA.

(**a**) BMDMs from WT, *Casp1*, *Asc*, *Nlrp3*, *Nlrc4*, *Aim2*, *Mefv*-deficient mice, or C-terminal pyrin-truncation mice (*Mefv*$^{\Delta Ct/\Delta Ct}$) were treated with LPS (1 μg/ml) and C3 toxin (0.5 μg/ml) for 6h. (**b**,**c**) BMDMs from WT mice were treated with LPS, C3 toxin, and the indicated concentration of (**b**) CNF toxin or (**c**) calpeptin for 6h. Cell culture supernatants were analyzed by IL-1β ELISA. ** $P \leq 0.005$ and *** $P \leq 0.0005$ (unpaired two-tailed *t*-test). Data represent the mean ± s.e.m from six independent experiments. (**d**,**e**) BMDMs from (**d**) WT mice were treated with LPS, C3 toxin, and calpeptin, or (**e**) *Mefv*$^{V726A/V726A}$ mice were co-treated with LPS and calpeptin for 6h and then analyzed for IL-1β release by immunoblotting. (**f**) BMDMs from WT mice were co-treated with LPS, the indicated concentration of calpeptin for 5h, and then ATP for 0.5h, flagellin for 1h, or dsDNA for 1h. Cell culture supernatants (Sup) and cell lysates (Lys) were analyzed by immunoblotting as indicated. All immunoblot data shown are representative of at least three independent experiments.

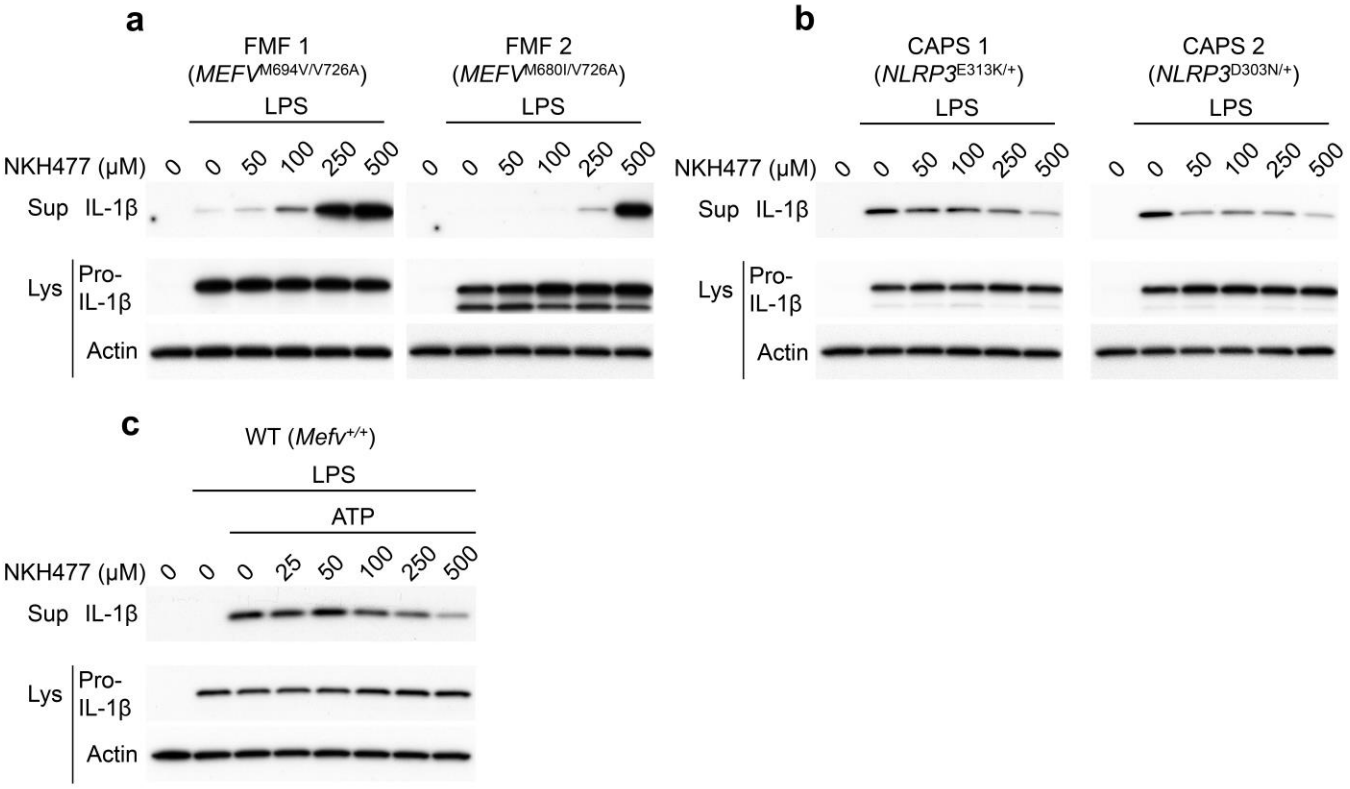

Supplementary Figure 2

cAMP suppresses NLRP3 inflammasome activation but potentiates pyrin inflammasome activation.

(**a**) PBMCs from FMF patients (designated patient number 1 and 2) with the indicated mutations in *MEFV* were non-primed or primed with LPS for 3h and then treated with the indicated dose of NKH477, a potent adenylate cyclase activator, for 1h. (**b**) PBMCs from CAPS patients (designated patient number 1 and 2) with the indicated mutations in *NLRP3* were non-primed or primed with LPS (1 μg/ml) for 3h and then treated with the indicated concentration of NKH477 for 1h. (**c**) BMDMs from WT mice were primed with LPS (1 μg/ml) for 3h and then treated with ATP (2 mM) and the indicated concentration of NKH477 for 0.5h. Cell culture supernatants and cell lysates were analyzed by immunoblotting as indicated. All immunoblot data shown are representative of at least three independent experiments.

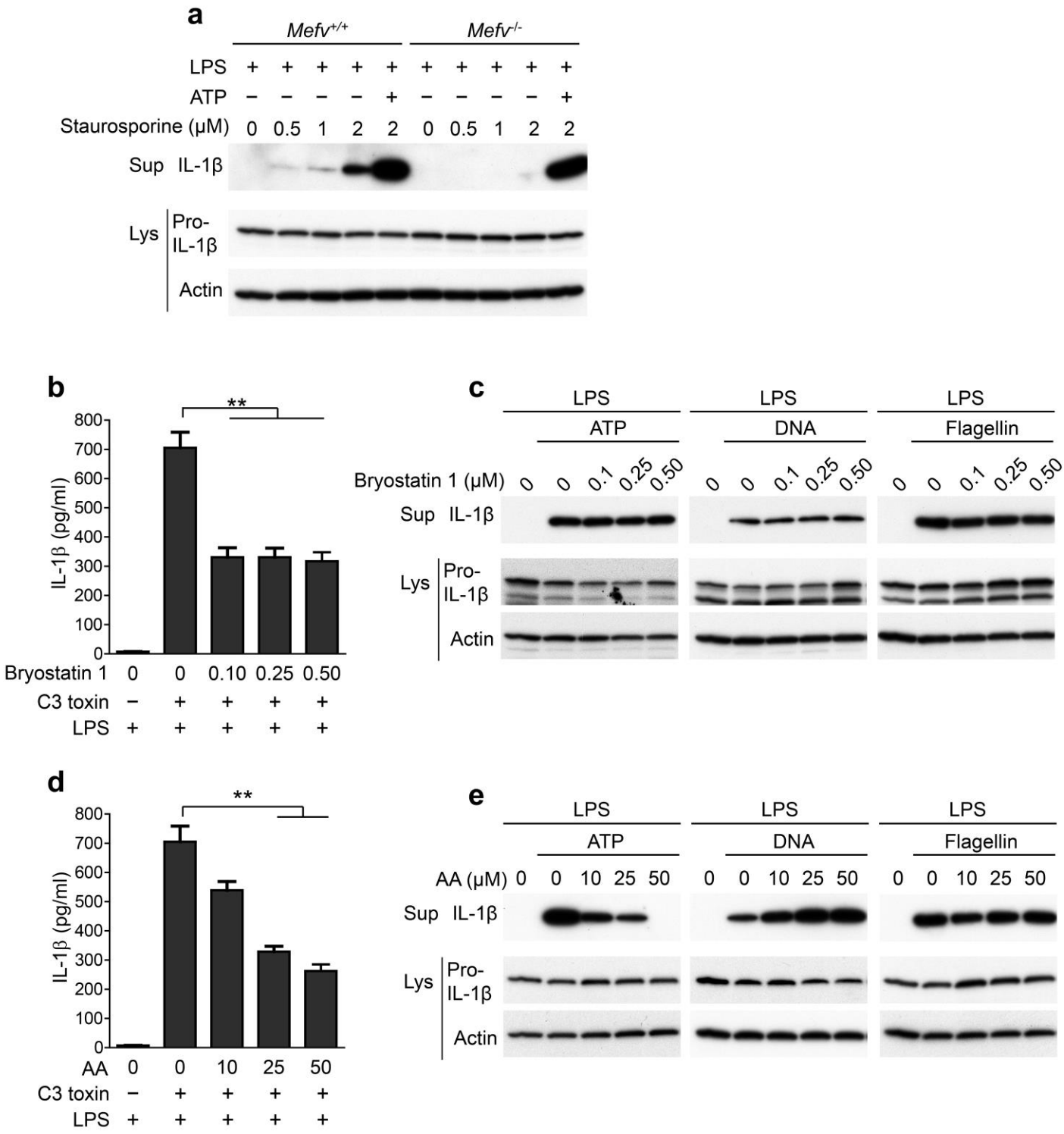

Supplementary Figure 3

RhoA effector kinases suppress pyrin inflammasome activation.

(**a**) LPS-primed BMDMs from WT or *Mefv*$^{-/-}$ mice were treated with the indicated dose of staurosporine or staurosporine (2 μM) and ATP

(2 mM). (**b**,**d**) BMDMs from WT mice were co-treated with LPS and the indicated concentration of (**b**) bryostatin 1 or (**d**) arachidonic acid (AA) with C3 toxin for 6h. Cell culture supernatants were analyzed by IL-1β ELISA. ** $P \leq 0.005$ (unpaired two-tailed *t*-test). Data represent the mean ± s.e.m from six independent experiments. (**c**,**e**) LPS-primed BMDMs from WT mice were treated with the indicated concentration of (**c**) bryostatin 1 or (**e**) arachidonic acid and ATP (2 mM) for 0.5h, dsDNA (1 µg/ml with 2.5 µl/ml of Lipofectamine 2000) for 1h, or flagellin (0.5 µg/ml with 25 µl/ml DOTAP) for 1h. Cell culture supernatants and cell lysates were analyzed by immunoblotting as indicated. All immunoblot data shown are representative of at least three independent experiments.

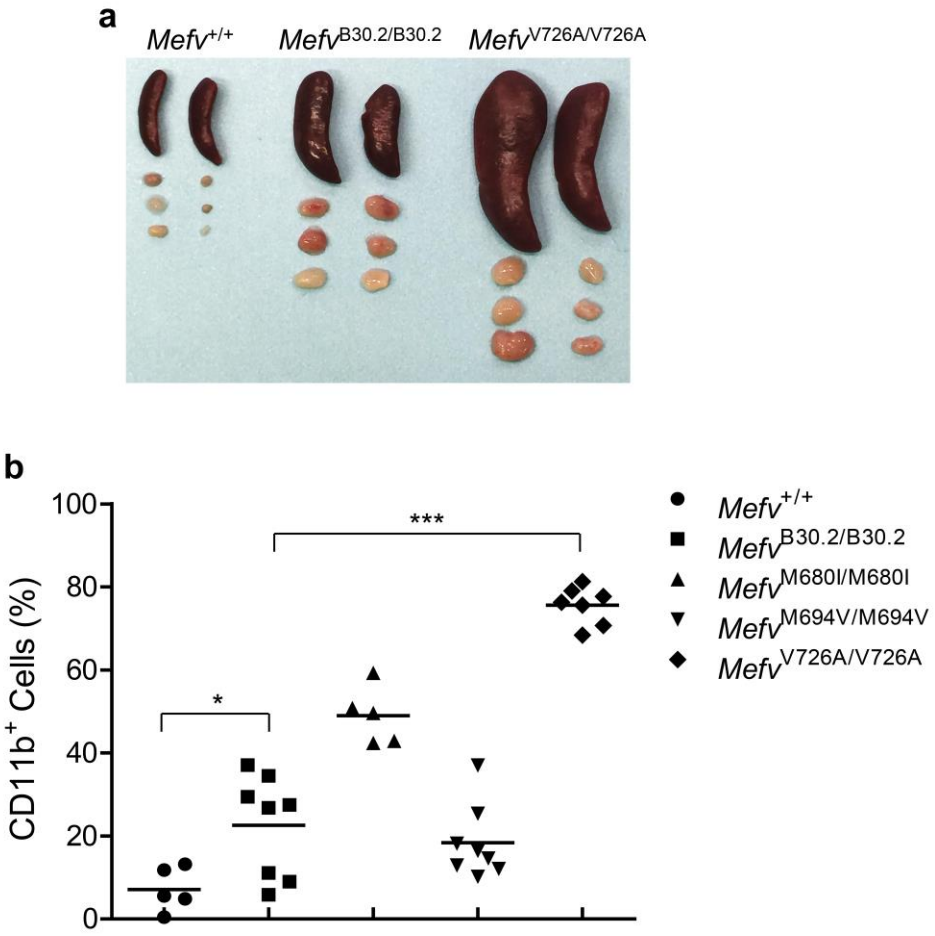

Supplementary Figure 4

Knock-in mice with the wild-type B30.2 domain of human pyrin have a milder inflammatory phenotype than that of knock-in mice with FMF-associated mutations.

(**a**) Lymphadenopathy and splenomegaly of FMF KI mice. The photograph shows lymph nodes and spleens from each of two 16 week-old *Mefv*$^{+/+}$, *Mefv*$^{B30.2/B30.2}$, and *Mefv*$^{V726A/V726A}$ mice. (**b**) Peripheral blood cells from *Mefv*$^{+/+}$, *Mefv*$^{B30.2/B30.2}$, *Mefv*$^{M680I/M680I}$, *Mefv*$^{M694V/M694V}$, and *Mefv*$^{V726A/V726A}$ mice were analyzed for CD11b^{+} myeloid cells. Numbers indicate percentage of total cells in gates. Each graph point represents one mouse, and means are shown as horizontal bars. * $P \leq 0.05$ and *** $P \leq 0.0005$ (unpaired two-tailed *t*-test).

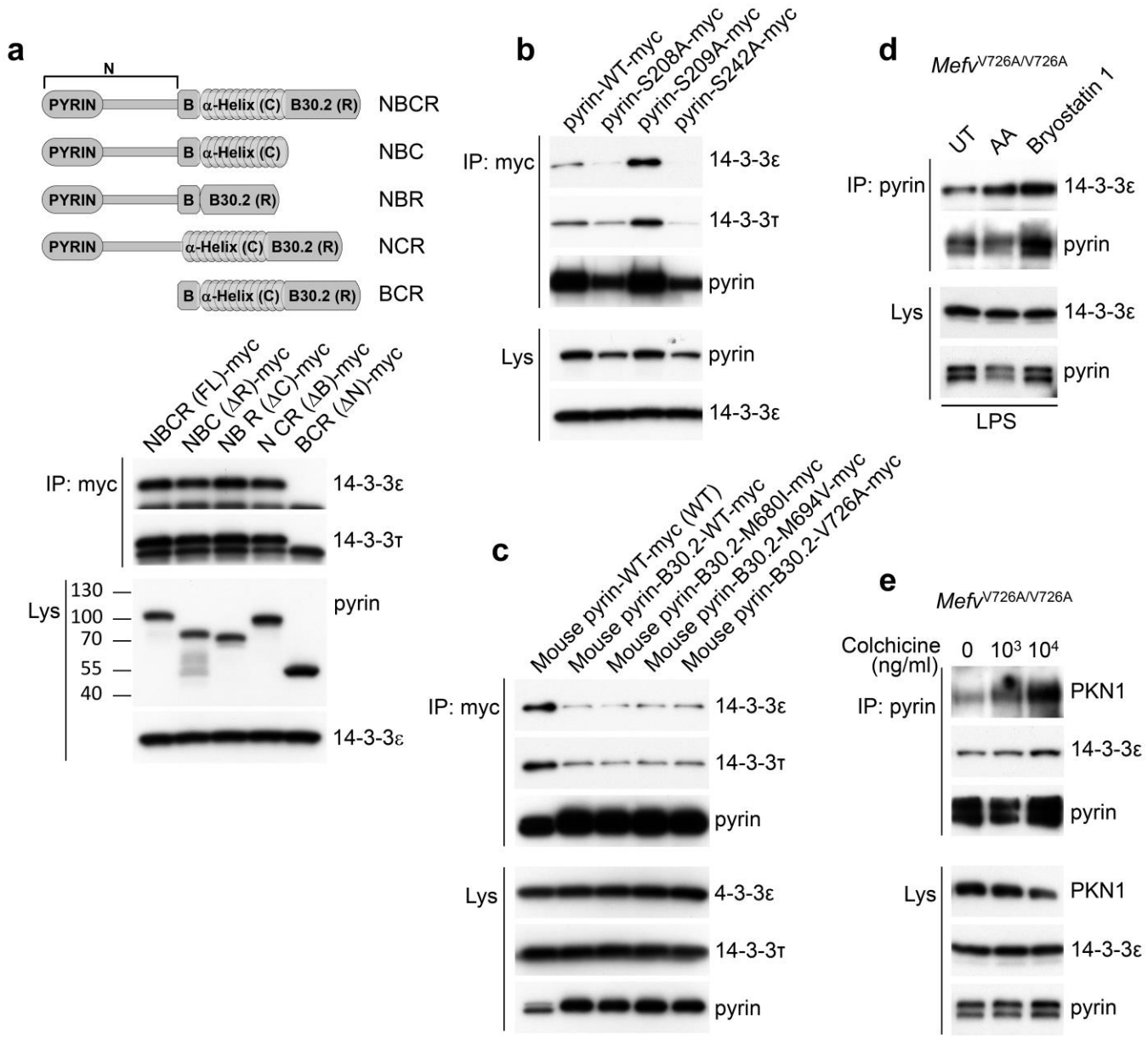

Supplementary Figure 5

14-3-3 proteins bind to pyrin.

(**a**) The lysates of 239T cells transiently expressing full length or various deleted forms of pyrin (top) were immunoprecipitated with anti-myc antibody and analyzed by immunoblot for 14-3-3 proteins (bottom). (**b**) The lysates of 239T cells transiently expressing myc-tagged WT or the indicated mutant pyrin proteins were immunoprecipitated with anti-myc antibody and analyzed by immunoblot for 14-3-3 proteins. (**c**) The lysates of PT67 cells transiently expressing WT mouse pyrin or the indicated human B30.2 domain-fused mouse pyrin were immunoprecipitated with anti-myc antibody and analyzed by immunoblot for 14-3-3 proteins. (**d**) BMDMs from *Mefv*$^{V726A/V726A}$ mice were co-treated with LPS and arachidonic acid or bryostatin 1. Cell lysates were immunoprecipitated with anti-pyrin antibody, and immune complexes were analyzed by immunoblot for 14-3-3ε and pyrin. (**e**) BMDMs from *Mefv*$^{V726A/V726A}$ mice were co-treated with LPS and the indicated concentration of colchicine. Cell lysates were immunoprecipitated with anti-pyrin antibody, and immune complexes were analyzed by immunoblot for PKN1, 14-3-3ε, and pyrin. All immunoblot data shown are representative of at least three independent experiments.

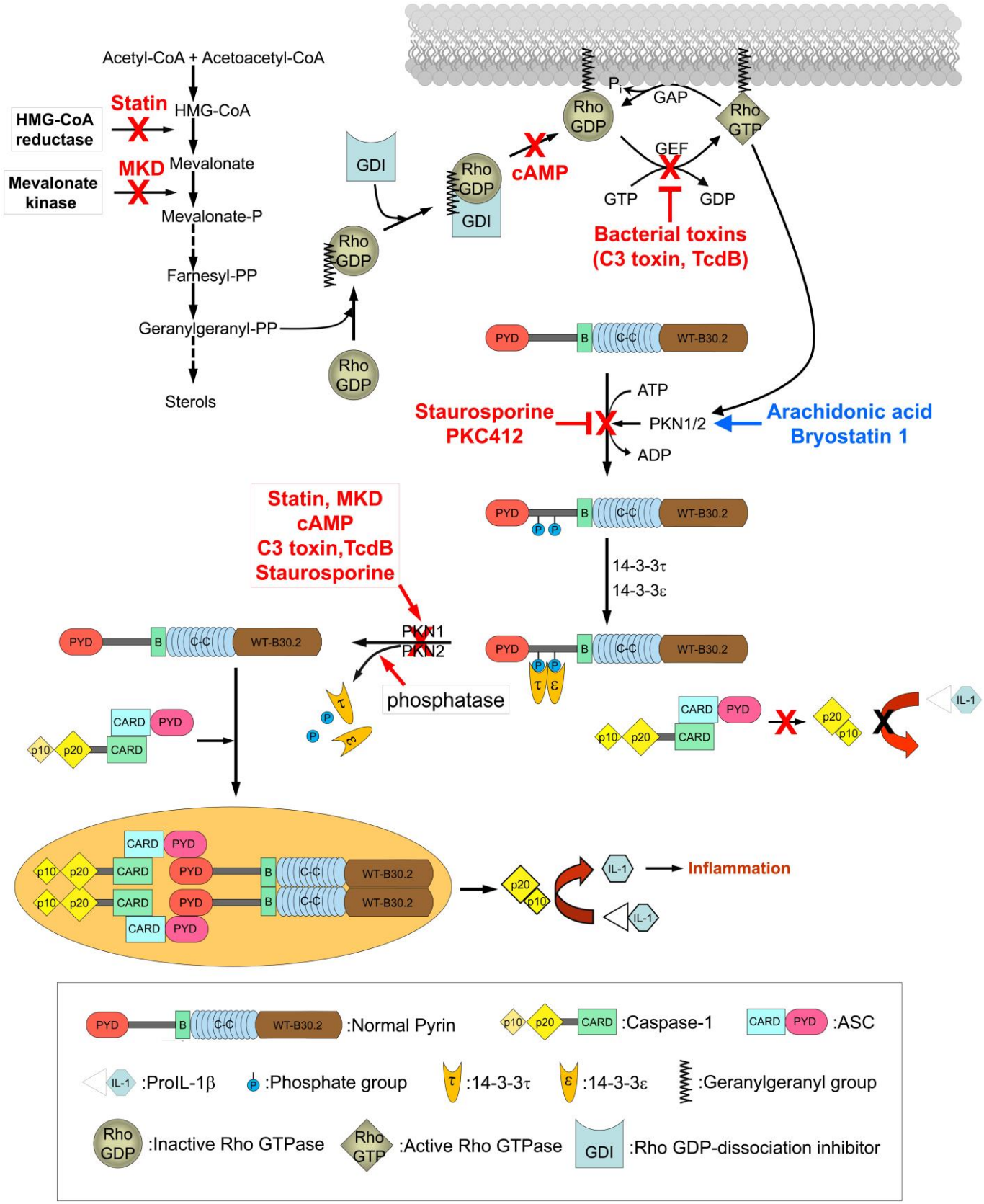

Nature Immunology: doi:10.1038/ni.3457

Supplementary Figure 6

Proposed molecular mechanism of pyrin inflammasome activation.

Inactivation of RhoA by bacterial toxin-mediated modification, cAMP-mediated phosphorylation, or a defect of geranylgeranylation that causes HIDS leads to inactivation of the RhoA effector kinases, PKN1 and PKN2. Inactivation of effector kinases results in dephosphorylation of pyrin by yet unknown phosphatases and 14-3-3 protein dissociation. Free pyrin activates caspase-1 through the formation of a pyrin inflammasome.

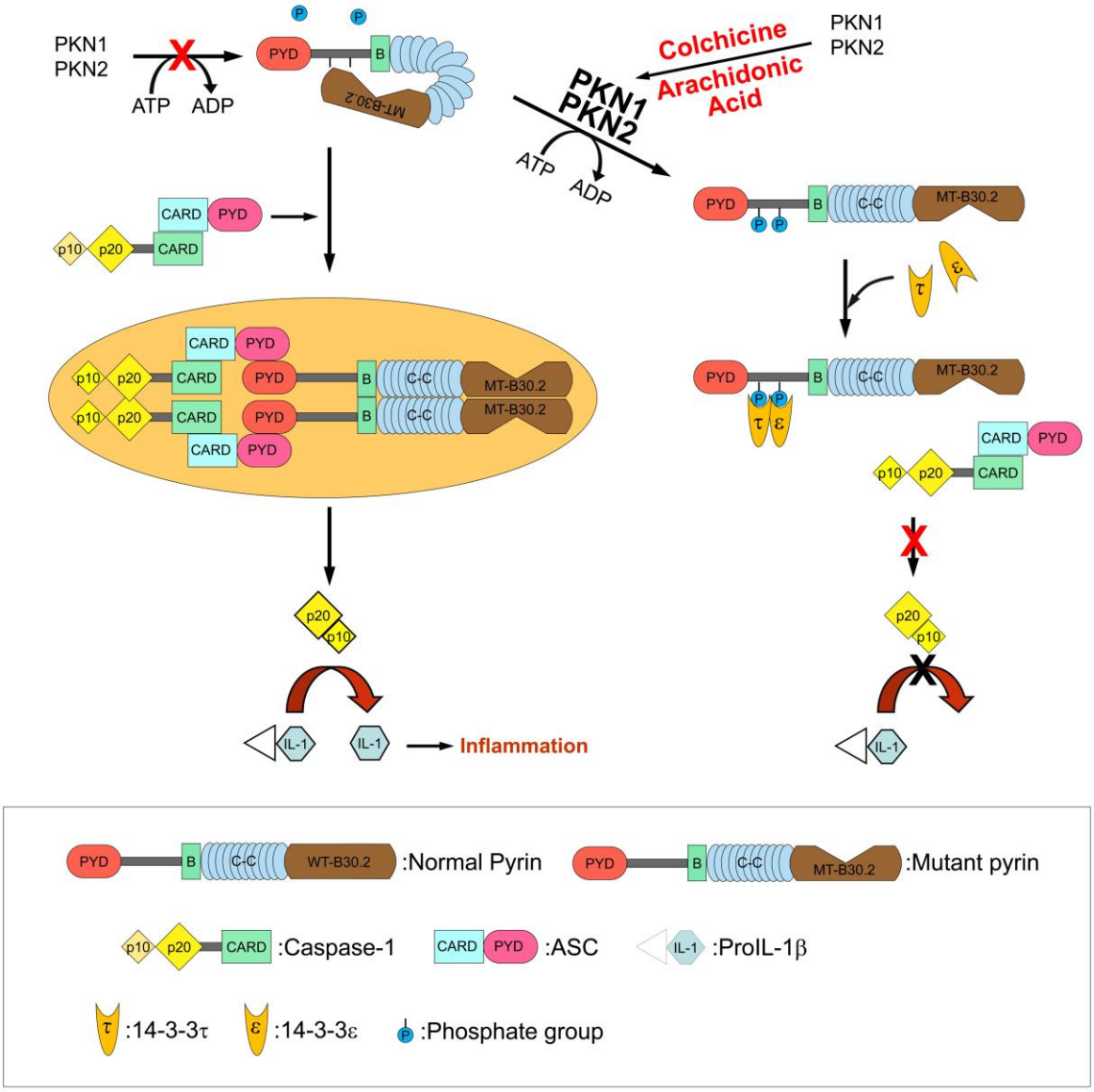

Supplementary Figure 7

Proposed molecular mechanism of pyrin inflammasome activation caused by FMF-associated mutant pyrin.

FMF-associated mutant B30.2 domain inhibits the binding of RhoA effector kinases onto pyrin, which results in decreased phosphorylation of pyrin, decreased 14-3-3 binding to pyrin, and the activation of the pyrin inflammasome. The pyrin inflammasome can be suppressed by RhoA effector kinase activators, such as colchicine or arachidonic acid.

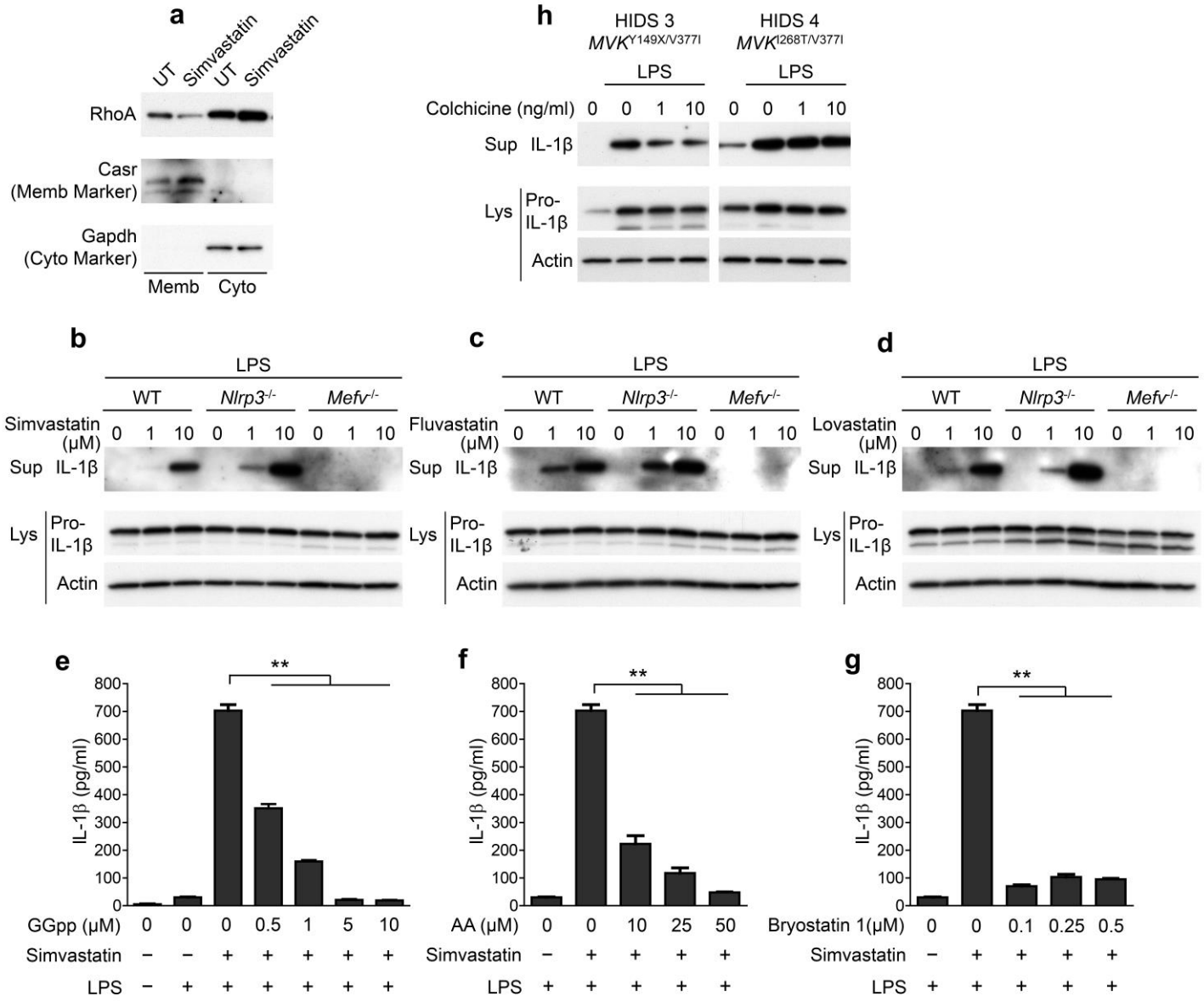

Supplementary Figure 8

HIDS is caused by the constitutive activation of the pyrin inflammasome.

(**a**) BMDMs from WT mice were treated with simvastatin (10 μM) for 16h and primed with LPS for 6h. Cell lysates were fractionated into membrane and cytosolic fractions, and analyzed by immunoblotting for RhoA. (**b-d**) BMDMs from WT, *Nlrp3*$^{-/-}$, or *Mefv*$^{-/-}$ mice were treated with the indicated concentration of (**b**) simvastatin, (**c**) fluvastatin, or (**d**) lovastatin for 16h and primed with LPS for 6h. Cell culture supernatants and cell lysates were analyzed by immunoblotting as indicated. (**e-g**) BMDMs from WT mice were treated with simvastatin for 16h and co-treated with LPS and the indicated concentration of (**e**) geranylgeranyl pyrophosphate (GGpp), (**f**) arachidonic acid, or (**g**) bryostatin 1 for 6h. Cell culture supernatants were analyzed by IL-1β ELISA. ** $P \leq 0.005$ (unpaired two-tailed *t*-test). Data represent the mean ± s.e.m from six independent experiments. (**h**) PBMCs from HIDS patients (designated patient number 3 and 4) with the indicated mutations in *MVK* were co-treated with LPS and the indicated concentration of colchicine for 6h. Cell culture supernatants and cell lysates were analyzed by immonoblotting as indicated. Immunoblot data shown are representative of one experiment (**h**) or at least three independent experiments (**a-d, h**).